

Faster photosynthetic induction in tobacco by expressing cyanobacterial flavodiiron proteins in chloroplasts

Rodrigo Gómez¹ · Néstor Carrillo¹ · María P. Morelli^{1,3} · Suresh Tula² · Fahimeh Shahinnia² · Mohammad-Reza Hajirezaei² · Anabella F. Lodeyro¹ 

Received: 26 April 2017 / Accepted: 26 September 2017
© Springer Science+Business Media B.V. 2017

Abstract Plants grown in the field experience sharp changes in irradiation due to shading effects caused by clouds, other leaves, etc. The excess of absorbed light energy is dissipated by a number of mechanisms including cyclic electron transport, photorespiration, and Mehler-type reactions. This protection is essential for survival but decreases photosynthetic efficiency. All phototrophs except angiosperms harbor flavodiiron proteins (Flvs) which relieve the excess of excitation energy on the photosynthetic electron transport chain by reducing oxygen directly to water. Introduction of cyanobacterial Flv1/Flv3 in tobacco chloroplasts resulted in transgenic plants that showed similar photosynthetic performance under steady-state illumination, but displayed faster recovery of various photosynthetic parameters, including electron transport and non-photochemical quenching during dark–light transitions. They also kept the electron transport chain in a more oxidized state and enhanced the proton motive force of dark-adapted leaves. The results

indicate that, by acting as electron sinks during light transitions, Flvs contribute to increase photosynthesis protection and efficiency under changing environmental conditions as those found by plants in the field.

Keywords Photosynthesis · Alternative electron transport · Flavodiiron proteins · Non-photochemical quenching · Dark–light transitions · Photosynthetic efficiency

Introduction

Oxygenic photosynthesis involves the function in tandem of two multi-subunit membrane-bound complexes, photosystems (PS) I and II, which provide the energy-transducing machinery to drive electrons against a thermodynamic gradient at the expense of light (Jagannathan et al. 2012). On one end of this linear photosynthetic electron transport (LET), the water-splitting system generates oxygen; on the opposite end, low-potential intermediates are produced in the form of NADPH and reduced ferredoxin to deliver hydride groups and electrons to metabolic routes responsible for C, N, and S assimilation, and to a plethora of dissipative and regulatory pathways (Pierella Karlusich et al. 2014). LET also generates a ΔpH across the thylakoid membrane which is used as an energy source for ATP synthesis (Kramer and Evans 2011). In their natural environments, plants are exposed to rapidly changing illumination conditions, and the use of light energy needs to be tightly controlled to prevent over-reduction of the photosynthetic electron transport chain (PETC) and photoinhibition under transient episodes of high irradiation. Alternative electron transports (AETs) are used to fulfill these tasks and to adjust the ATP/NADPH ratio and the ΔpH magnitude to the requirements of assimilatory

Electronic supplementary material The online version of this article (doi:10.1007/s11120-017-0449-9) contains supplementary material, which is available to authorized users.

✉ Anabella F. Lodeyro
lodeyro@ibr-conicet.gov.ar

- ¹ Instituto de Biología Molecular y Celular de Rosario (IBR-UNR/CONICET), Facultad de Ciencias Bioquímicas y Farmacéuticas, Universidad Nacional de Rosario (UNR), 2000 Rosario, Argentina
- ² Leibniz Institute of Plant Genetics and Crop Plant Research, OT Gatersleben, Corrensstrasse, 06466 Stadt Seeland, Germany
- ³ Present Address: Departamento de Química Biológica (QB 23), Facultad de Ciencias Exactas y Naturales, Universidad de Buenos Aires (UBA), C1428EGA Buenos Aires, Argentina

routes. The most widely employed among them is cyclic electron transport (CET) around PSI, which is mediated by ferredoxin via PGR5/PGRL1 and/or NAD(P)H dehydrogenase-like pathways (Yamori and Shikanai 2016) producing ATP without NADP⁺ reduction.

Oxygen photoreduction at PSI provides an additional electron sink to dissipate the excess of excitation energy over the PETC through the Mehler reaction and the water–water cycle (Asada 1999). Since this pathway resembles CET in the sense that it involves ATP synthesis without NADPH production, it is also termed pseudocyclic electron transport (Allahverdiyeva et al. 2015; Yamamoto et al. 2016). Photorespiration is still another dissipative route available in C3 plants (Hagemann et al. 2013). Finally, photosynthetic microorganisms, non-vascular plants, and gymnosperms harbor a different type of AET based on the activity of a family of enzymes called flavodiiron proteins (Flvs), which are able to reduce oxygen directly to water (Allahverdiyeva et al. 2015; Gerotto et al. 2016; Ilík et al. 2017; Shimakawa et al. 2017). Flvs are also found in non-photosynthetic prokaryotes, Archaea, and some anaerobic pathogenic protozoa, but not in angiosperms (Allahverdiyeva et al. 2015; Ilík et al. 2017). They share a common core composed of two redox centers: an N-terminal β -lactamase-like domain containing a non-heme catalytic Fe–Fe center and a C-terminal flavodoxin-like domain binding an FMN cofactor. Cyanobacterial and plant Flvs have acquired an extra C-terminal NAD(P)H-flavin reductase domain with FAD/FMN as a prosthetic group, thereby enabling them to use NAD(P)H as an electron donor (Vicente et al. 2008; Allahverdiyeva et al. 2015). Indeed, recombinant cyanobacterial Flvs displayed low NAD(P)H-dependent oxygenase and diaphorase activities in vitro (Vicente et al. 2002; Shimakawa et al. 2017). Some α -cyanobacteria and algae possess only two putative Flvs (Flv1 and Flv3), whereas β -cyanobacteria harbor four isoforms (Flv1–Flv4). They have been reported to act as heterodimers, with the pairs Flv1/Flv3 and Flv2/Flv4 being the functional species in vivo (Allahverdiyeva et al. 2015). Heterocyst-forming cyanobacteria still contain two other isoforms (Flv1B and Flv3B) which accumulate specifically in that compartment and participate in O₂ elimination, allowing N₂ fixation by oxygen-sensitive nitrogenase (Ermakova et al. 2013). Flv1/Flv3 and Flv2/Flv4 from the β -cyanobacterium *Synechocystis* PCC6803 have been the most extensively studied through a combination of biochemical, biophysical, and genetic approaches (Allahverdiyeva et al. 2015).

In addition to driving ATP synthesis, acidification of the lumen during build-up of Δ pH across the thylakoid membrane serves to down-regulate electron transport and to dissipate the excess of light energy absorbed by PSII chlorophylls as heat, a process monitored by the non-photochemical quenching (NPQ) of chlorophyll fluorescence (Müller et al. 2001). Once the light stress situation subsides,

photosynthetic activity requires some time to resume. Then, NPQ provides photoprotection at the expense of photosynthetic efficiency. This detrimental effect can be significant under field conditions, where plant canopies experience sharp fluctuations in the levels of absorbed light during daytime (Külheim et al. 2002). The contribution of the various alternative electron transports to regulation of the ATP/NADPH ratio and Δ pH (hence, to NPQ) varies among organisms. Angiosperms, which lack Flvs (Ilík et al. 2017), largely rely on PGR5/PGRL1-dependent CET for relieving the excess of excitation on the PETC (Shirao et al. 2013). Expression of Flv homologs from the moss *Physcomitrella patens* (FlvA and FlvB) in a *pgr5* mutant of *Arabidopsis* partially restored the wild-type (WT) phenotype (Yamamoto et al. 2016). When expressed in a WT background, however, Flvs did not compete with CET during steady-state photosynthesis, but contributed to PS protection under fluctuating light and allowed for faster recovery from dark adaptation (Yamamoto et al. 2016).

The aim of this article is thus twofold: (a) to determine if Flv1 and Flv3 from *Synechocystis*, the best studied of all Flvs, could mediate electron transfer from the PETC to oxygen when expressed in plants as done by their *Physcomitrella* counterparts, and (b) to characterize the contribution of this electron sink for photosynthetic dark recovery. Tobacco plants co-expressing *Synechocystis* Flv1 and Flv3 in chloroplasts displayed faster photosynthetic electron transport at dark–light transitions, increasing NPQ and the oxidation state of the PETC. The effect of this AET was largely accounted for by improved dissipation of excess light energy via mechanisms depending on the establishment of a higher proton gradient across the thylakoid membrane. The results shown here indicate that Flvs could enhance photosynthetic efficiency of plants exposed to sudden changes in light intensity even in the presence of other dissipative systems.

Materials and methods

Construction of binary plasmids, tobacco transformation, and plant growth conditions

Plasmid pCHF3-FLV1-FLV3, containing the *flv1* (sl11521) and *flv3* (sl10550) genes from *Synechocystis* sp. PCC6803, each fused in-frame to a 5'-terminal sequence encoding the transit peptide (TP) of pea ferredoxin-NADP⁺ reductase (FNR), and placed under the control of individual CaMV-35S promoters, was constructed in a multiple-step approach using restriction enzymes and the Gibson assembly kit (NEB), according to the manufacturer's instructions. Cyanobacterial genes were amplified from *Synechocystis* genomic DNA by PCR using high-fidelity Phusion DNA

polymerase (NEB) and oligonucleotides listed in Supplementary Table S1. The recombinant plasmid prepared by Giró et al. (2011) was used as the source of TP by removing the DNA fragment coding for the mature sequence of FNR with *SalI* and *SacI*, and replacing it with the *flv1* coding region amplified with primers UP1F and UP1RV (Supplementary Table S1), resulting in pUC-TP-FLV1. The TP-*flv1* coding region was amplified from pUC-TP-FLV1 with primers CH1F and CH1RV (Supplementary Table S1) and inserted in a pCHF3 vector (Jarvis et al. 1998) digested with *SalI* and *SacI*. The resulting plasmid (pCHF3-TP-FLV1) contained the TP-FLV1 sequence between a CaMV-35S promoter and a terminator/polyadenylation signal from the pea *rbcS-E9* gene.

Plasmid pCHF3-TP-FLV3 was obtained from pCHF3-TP-FLV1 by replacing the *SacI-SalI flv1* fragment with the *flv3* coding sequence using primers CH3F and CH3RV (Supplementary Table S1). Finally, the pCHF3-FLV1-FLV3 plasmid was prepared by inserting the fragment spanning the CaMV-35S promoter, the TP-*flv3* sequences, and the *rbcS-E9* terminator, amplified from pCHF3-TP-FLV3 with primers DOB-F and DOB-RV (Supplementary Table S1), into pCHF3-TP-FLV1 digested with *Bam*HI. Inserted fragments in pCHF3-FLV1-FLV3 (Fig. 1a) were confirmed by DNA sequencing (UMaine DNA facility, US). The resulting plasmid was introduced into the genome of *Nicotiana tabacum* cv. Petit Havana through *Agrobacterium tumefaciens*-mediated leaf disk transformation (Gallois and Marinho 1995). Selection of transformants and segregation analysis were based on kanamycin resistance. Primary transformants were self-pollinated and all subsequent experiments were carried out with the homozygous progeny. Seeds were germinated on 0.8% (w/w) agar (Sigma) containing half-strength Murashige–Skoog basal salts (Sigma), and in the case of transformants, 100 $\mu\text{g mL}^{-1}$ kanamycin. After 3 weeks,

seedlings were transferred to soil, watered daily, and grown at 200 $\mu\text{mol photons m}^{-2} \text{ s}^{-1}$, 25 °C, and a 16/8-h photoperiod (growth chamber conditions).

RNA extraction, cDNA synthesis, and real-time quantitative reverse transcription PCR (qRT-PCR) reactions

Total RNA was isolated from the third and fourth fully expanded leaves of 8-week-old plants using TriPure reagent (Roche Sigma-Aldrich) according to the manufacturer's instructions, and treated with RNase-free DNase I (Promega) prior to cDNA synthesis using oligo d(T)₁₄ and M-MLV reverse transcriptase (Invitrogen). Quantitative RT-PCR assays were performed in a Mastercycler_ep realplex thermal cycler (Eppendorf) using Platinum Taq DNA polymerase (Invitrogen) and SYBR Green I (Roche) to monitor the synthesis of double-stranded DNA. Relative transcript levels were determined for each sample by the ΔCt method (Schmittgen and Livak 2008), using primers listed in Supplementary Table S1 for *flv1* (qF1f and qF1rv) and *flv3* (qF3f and qF3rv), and normalized against the levels of EF1 α cDNA encoding elongation factor 1 (accession number: AF120093) with primers EF1f and EF1v (Supplementary Table S1). PCR amplification efficiencies for each pair of primers were close to two as determined by serial dilution curves (Schmittgen and Livak 2008).

Photosynthetic measurements

Pulse-amplitude modulation (PAM) fluorometry, chlorophyll content (SPAD), and total electrochromic shift (ECSt) measurements were carried out using a MultispeQ-Beta device controlled by the PhotosynQ platform software (Kuhlgert et al. 2016). Measurements were carried out on the third and

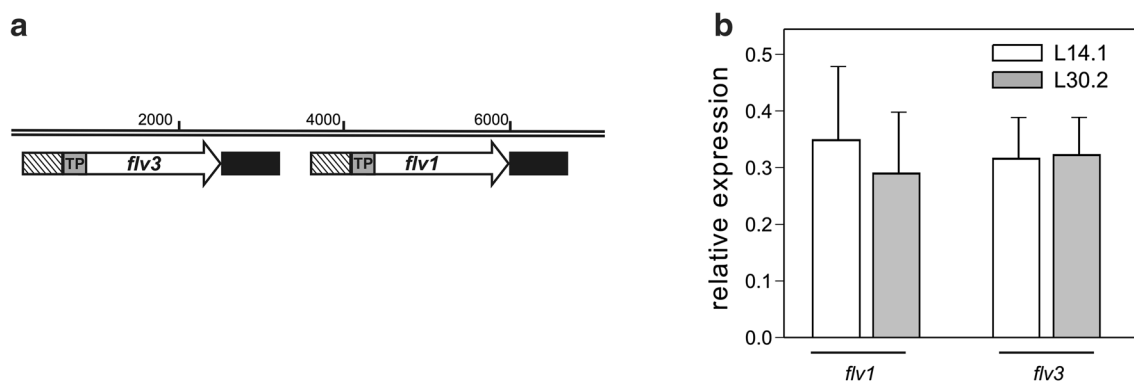


Fig. 1 Expression of cyanobacterial flavodiiron proteins in tobacco plants. **a** Schematic representation of the T-DNA fragment of the pCHF3-FLV1-FLV3 plasmid containing the *flv3* and *flv1* (white arrows) and pea FNR TP coding sequences (gray boxes), CaMV35S promoters (striped boxes), and rbsS-E9 terminator sequences (black

boxes). **b** Levels of *flv1* and *flv3* transcripts in transgenic lines L14.1 (white bars) and L30.2 (gray bars), as determined by qRT-PCR relative to EF1 α . Bars show mean values \pm SE obtained from four plants for each independent line, with technical triplicates

fourth fully expanded leaves of 8-week-old plants, subjected to at least 2 h of previous dark adaptation to inactivate the Calvin–Benson cycle. Actinic illumination and short saturation pulses ($3000 \mu\text{mol photons m}^{-2} \text{s}^{-1}$, 500 ms) were provided by a red LED (emission peak at 650 nm). Photosynthetic induction parameters were derived from chlorophyll fluorescence transients measured on dark-adapted leaves: initial basal fluorescence (F_0) and maximal fluorescence with a saturation pulse (F_m) were recorded before turning on the actinic light (250 and $1000 \mu\text{mol photons m}^{-2} \text{s}^{-1}$). During the illumination period, eight saturation pulses were applied, separated from each other by 5-s intervals. The same results were obtained when applying the saturation pulses at different time intervals (5–20 s), indicating the absence of actinic effects caused by the string of pulses. All parameters were calculated using equations described by Kramer et al. (2004).

NPQ relaxation analysis was performed on dark-adapted leaves: F_0 and F_m were recorded prior to illumination with actinic light of $250 \mu\text{mol photons m}^{-2} \text{s}^{-1}$ for 5 min, followed by a 5-min period of darkness. Saturation pulses were applied after 40 s of illumination and at the end of dark period, and the resulting fluorescence transients used to calculate the Φ_{qE} and Φ_{qT+qI} parameters as described by Ahn et al. (2009).

The total electrochromic shift (ECSt) during light–dark transitions was determined by the absorbance change at 525 nm induced by 300 ms of dark intervals. The proton motive force was estimated on dark-adapted leaves after different periods of illumination ($250 \mu\text{mol photons m}^{-2} \text{s}^{-1}$ at 650 nm), as the total amplitude of the light–dark ECSt. These values were normalized against the ΔA_{525} induced by a single-turn-over flash (ECSst) on dark-adapted leaves before turning on the actinic light, in order to account for differences in leaf thickness and chloroplast density.

CO_2 assimilation rates (A) were measured with a LI-6200 (Licor Biosciences) under steady-state illumination with a PAR intensity of $200 \mu\text{mol m}^{-2} \text{s}^{-1}$.

Antimycin A treatment

To inactivate the main CET activity depending on PGR5/PGR1, leaf disks (12-mm diameter) from 8-week-old plants were placed into Petri dishes between moist tissue papers soaked with $10 \mu\text{M}$ antimycin A or water as control. Disks were incubated for 12 h in the dark before measurements.

Statistical analyses

Results were expressed as means \pm SE. Statistical significance was determined by ANOVA for multiple comparison analyses followed by post hoc Tukey's HSD test when

needed, using StatGraphics plus 5.0 (<https://statgraphics.softonic.com/>).

Results

Since Flv1 and Flv3 are expected to function as a heterodimeric unit, *Synechocystis* genes encoding these proteins were expressed simultaneously using the pCHF3-FLV1-FLV3 plasmid (Fig. 1a; see also “Materials and methods”). Transgenic plants were able to grow and set seeds, from which homozygous lines were selected. Two independent lines (L14.1 and L30.2) were employed in further experiments. Expression of the transgenes was followed by qRT-PCR, which showed that the two transcripts accumulated in the transgenic lines (Fig. 1b). The transgenic plants did not display phenotypic differences with their WT siblings when grown under growth chamber conditions, in terms of biomass, CO_2 assimilation rates, maximal PSII efficiency (F_v/F_m), and leaf pigments (Supplementary Table S2). The Flv-expressing lines were used to study photosynthesis induction at the onset of illumination by measuring the time course of several photosynthetic parameters after exposure of dark-adapted leaves to two light intensities (250 and $1000 \mu\text{mol photons m}^{-2} \text{s}^{-1}$).

The quantum yield of PSII (Φ_{PSII}) was determined to estimate the rates of LET (Baker 2008), whereas its maximal value, represented by the F_v/F_m ratio, was used to monitor photodamage to PSII (Baker 2008). While the F_v/F_m values of WT and Flv-expressing plants were not statistically different (Supplementary Table S2), the average Φ_{PSII} values were more than twofold higher in Flv-expressing plants compared to the wild type immediately after illumination with $250 \mu\text{mol photons m}^{-2} \text{s}^{-1}$ (Fig. 2a). The Φ_{PSII} values were significantly lower, as expected, when the light intensity was raised to $1000 \mu\text{mol photons m}^{-2} \text{s}^{-1}$, but the effect of Flv1/Flv3 expression was still evident (Fig. 2b). The Φ_{PSII} gap between WT and Flv leaves decreased steadily with time (Fig. 2a, b), concurring with the observation that Flv expression in *Arabidopsis* had little or no effect on steady-state photosynthesis (Yamamoto et al. 2016). The qL parameter, which estimates the fraction of photochemically active PSII reaction centers, displayed a similar behavior (Fig. 2c, d), indicating a higher oxidation state of the PETC in the transgenic plants from the beginning of the illumination period. Taken together, the Φ_{PSII} and qL responses indicate the existence of a larger electron sink in *flv1/flv3* lines. In addition, NPQ was higher in Flv-expressing plants during the induction period under the illumination intensities of 250 and $1000 \mu\text{mol photons m}^{-2} \text{s}^{-1}$ (Fig. 3a, b). Differences between WT and transgenic lines were no longer detected after photosynthesis reached the steady-state conditions (Supplementary Fig. S1).

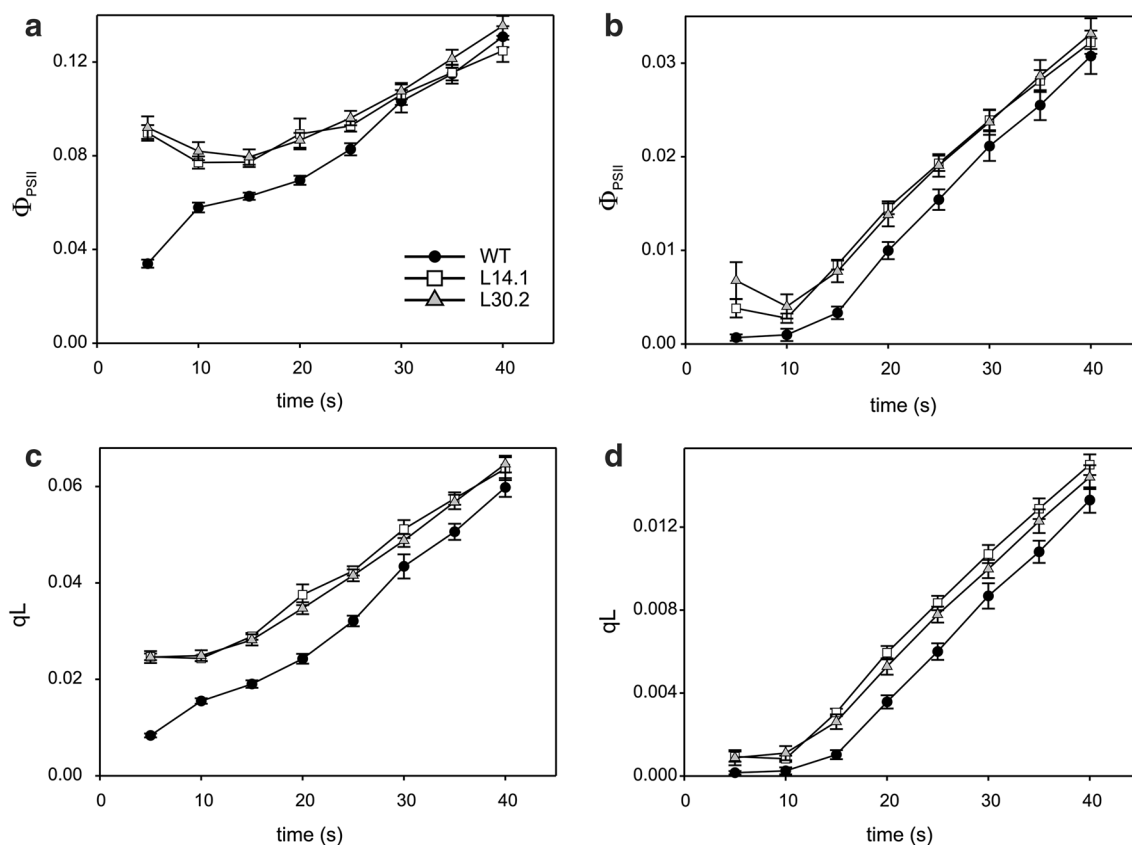


Fig. 2 Flv-dependent improvement of the PSII quantum yield and oxidation state of PETC over the first 40 s of photosynthesis induction. The Φ_{PSII} (a, b) and qL (c, d) values were determined at 250 $\mu\text{mol photons m}^{-2} \text{s}^{-1}$ (a, c) or 1000 $\mu\text{mol photons m}^{-2} \text{s}^{-1}$ (b, d)

To distinguish between the various mechanisms of non-photochemical energy dissipation that could be affected by Flv presence, we estimated the Φ_{NPQ} and Φ_{NO} parameters, corresponding to the quantum yields of light-induced and basal dissipative processes, respectively (Kramer et al. 2004). As illustrated in Fig. 3c–f, Φ_{NPQ} was higher and Φ_{NO} lower in the transgenic plants relative to the wild type at both light intensities. These results indicate that the presence of Flv1/Flv3 favored light-dependent dissipative processes at the expense of mechanisms related to fluorescence and interconversion of triplet-state chlorophyll. Then, this effect should mitigate the propagation of reactive oxygen species resulting from energy transfer at PSII (Ahn et al. 2009).

To further characterize the contribution of Flvs to modulation of the excitation energy on the PETC, the major CET activity depending on PGR5/PGRL1 was inactivated using antimycin A (Joët et al. 2001; Sugimoto et al. 2013). Typical results obtained with lines L14.1 and L30.2 are illustrated in Fig. 4 and Supplementary Fig. S2, respectively. WT leaf disks incubated with 10 μM antimycin A for 16 h in the dark exhibited a significant decline of Φ_{PSII} and qL upon illumination (Fig. 4a, b; Supplementary Fig. S2a, b). While Φ_{PSII}

of actinic light illumination on dark-adapted leaves of WT (black circles) and Flv1/Flv3-expressing lines L14.1 (white squares) and L30.2 (gray triangles). Results are expressed as means \pm SE, $n > 10$

and qL increased with time for both antimycin-treated and control disks, the differences between them actually widened (Fig. 4a, b; Supplementary Fig. S2a, b). The inhibitory effect of antimycin A on Φ_{PSII} and qL was attenuated in leaves expressing Flv1/Flv3 (Fig. 4a, b; Supplementary Fig. S2a, b). This compensation was also evident in dissipative processes, with almost full preservation of NPQ, Φ_{NPQ} , and Φ_{NO} (Fig. 4c–e; Supplementary Fig. S2c–e), indicating that Flv-dependent electron transport to oxygen was able to take over the functions of CET when the PGR5/PGRL1 pathway was inactivated.

To identify which light-regulated mechanisms preferentially contribute to the differential increase of Φ_{NPQ} at the onset of the illumination period in Flv-expressing plants, we determined Φ_{qE} and $\Phi_{\text{qT+qI}}$ values by NPQ relaxation analysis. The first of these parameters is associated to fast relaxing processes depending on the generation of a proton gradient across the thylakoid membrane, and the second to processes displaying slower relaxation, mainly through transition-state quenching and PSII photoinhibition. These latter processes, as estimated through $\Phi_{\text{qT+qI}}$, did not differ between WT and transgenic plants, whereas the Φ_{qE}

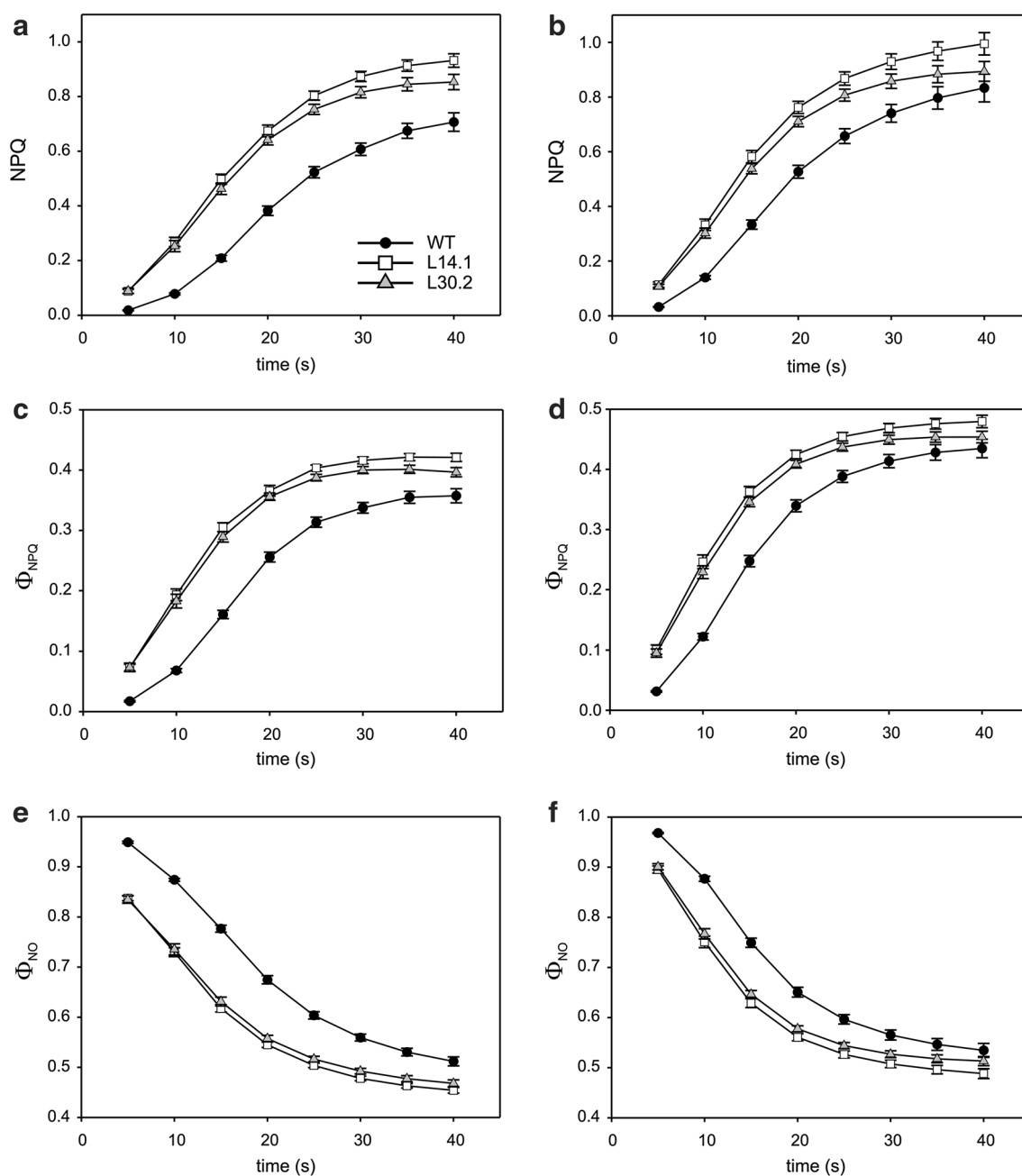


Fig. 3 Faster non-photochemical quenching generation in Flv-expressing tobacco plants during the induction period of photosynthesis. NPQ (**a**, **b**), Φ_{NPQ} (**c**, **d**), and Φ_{NO} (**e**, **f**) of dark-adapted WT (black circles) and Flv-expressing lines L14.1 (white squares) and

L30.2 (gray triangles) were measured on leaves illuminated with actinic light at 250 $\mu\text{mol photons m}^{-2} \text{s}^{-1}$ (**a**, **b**, **e**) or 1000 $\mu\text{mol photons m}^{-2} \text{s}^{-1}$ (**b**, **d**, **f**). Results are expressed as means \pm SE, $n > 10$

parameter was significantly higher in leaf tissue expressing Flvs (Fig. 5), indicating that Flv1/Flv3 contributed to the establishment of ΔpH across the thylakoid membrane in the transformants.

In agreement with these observations, the increase of the thylakoid proton motive force (PMF) of dark-adapted leaves upon illumination, estimated via ECS

measurements, was significantly faster in the transgenic lines than in their WT counterparts (Fig. 6). Once the steady state was reached, after up to 300 s of illumination, WT and Flv-expressing plants showed no differences in PMF values (Fig. 6). Then, the results agree well with the fast establishment of light-dependent non-photochemical dissipation via NPQ and Φ_{NPQ} (Fig. 3).

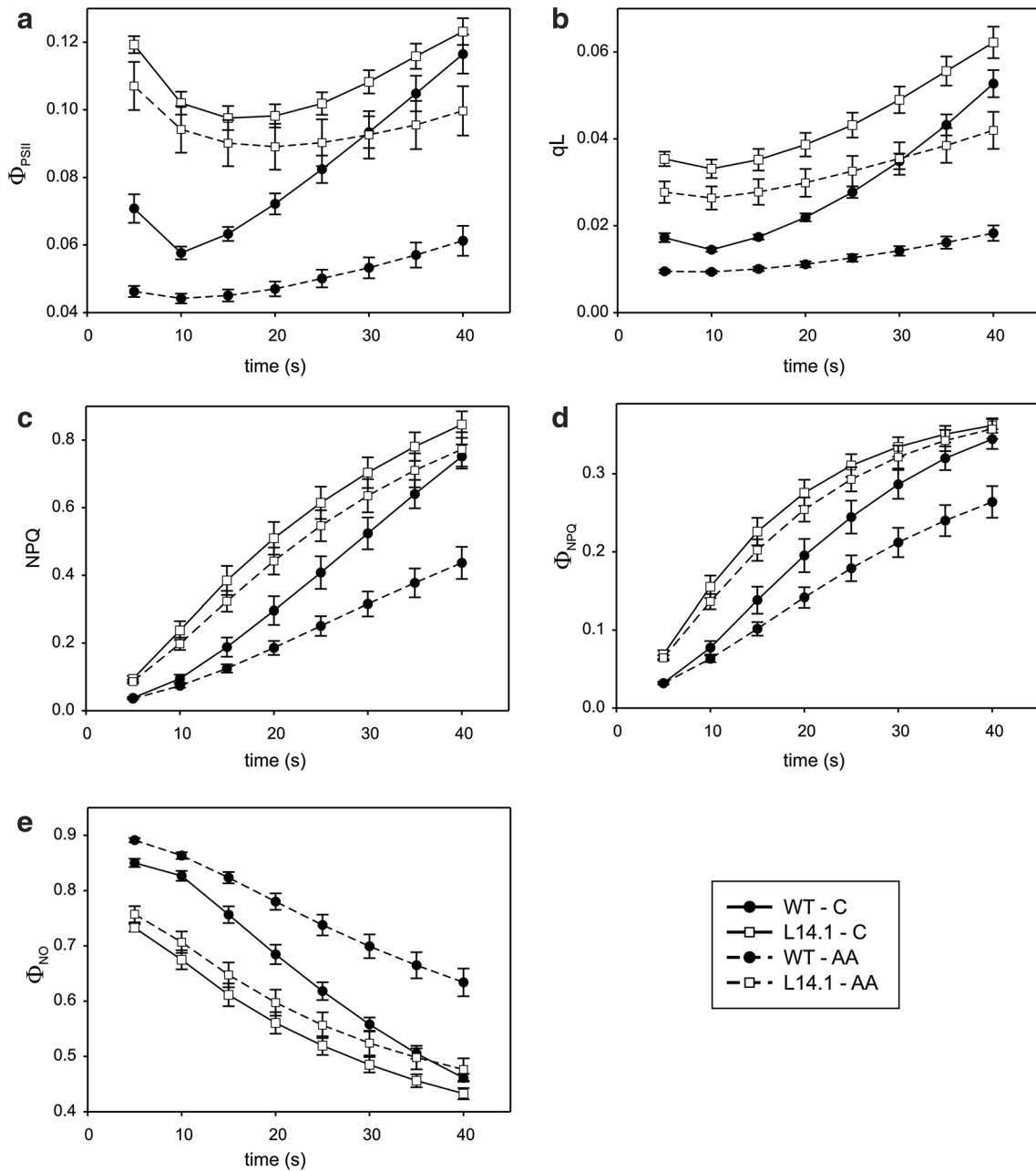


Fig. 4 Protective effects of Flv expression on antimycin A-treated leaf disks. **a** Φ_{PSII} , **b** qL , **c** NPQ, **d** Φ_{NPQ} , and **e** Φ_{NO} values were determined during photosynthesis induction at $250 \mu\text{mol photons m}^{-2} \text{s}^{-1}$ of WT leaf disks treated (WT—AA, black circles and dashed lines) or not (WT—C, black circles and continuous lines)

with $10 \mu\text{M}$ antimycin A, and L14.1 disks treated (L14.1—AA, white squares and dashed lines) or not (L14.1—C, white squares and continuous lines) with $10 \mu\text{M}$ antimycin A. Results are expressed as means \pm SE, $n=8$

Discussion

Illumination of plant canopies in the field varies widely during the day, with dynamic light transitions in various time-scales caused by clouds, other leaves, or changes in sun angles. When light intensity increases too fast for photochemical processes to use the absorbed energy, plants

induce protective mechanisms to prevent photo-oxidation of antennae complexes (Takahashi and Badger 2011). NPQ is one of the most important, allowing dissipation of the excess of excitation energy at PSII as heat (Duffy and Ruban 2015). Photosynthetic activity is down-regulated during this process, and requires some time to recover after the light stress has subsided. A key component of the

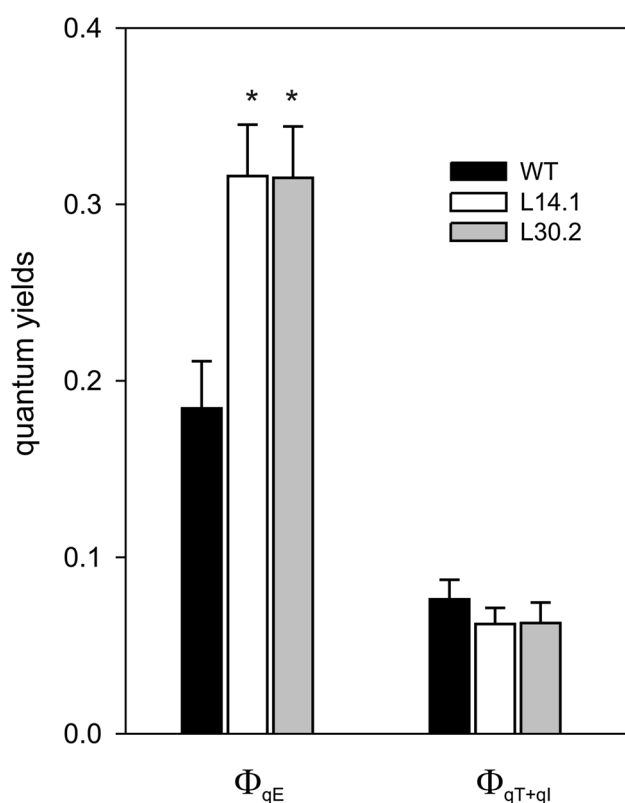


Fig. 5 Enhancement of fast relaxing processes of non-photochemical quenching in Flv-expressing tobacco plants determined by NPQ relaxation analysis. Quantum yield of fast (Φ_{qE}) and slow (Φ_{qT+qL}) relaxing processes contributing to NPQ were measured on WT (black bars) and Flv-expressing L14.1 (white bars) and L30.2 (gray bars) dark-adapted tobacco leaves. Results are expressed as means \pm SE, $n=6$. The asterisk indicates significant differences ($p < 0.05$)

feedback regulatory system of photosynthesis, essential for plants growing at fluctuating illumination and/or low CO_2 levels, is lumen acidification. It induces energy-dependent NPQ at PSII and regulates plastoquinol oxidation by the cytochrome *b₆f* complex, thus preventing downstream accumulation of electrons at PSI and subsequent photodamage (Nishio and Whitmarsh 1993; Hope et al. 1994).

Model simulations indicate that plants grown under fluctuating light could decrease CO_2 assimilation up to 20% compared to steady-state light conditions (Zhu et al. 2004). These predictions were confirmed experimentally in transgenic tobacco lines termed VPZ, which over-expressed three gene products reported to contribute to fast NPQ induction and relaxation during light–dark transitions (Kromdijk et al. 2016). VPZ plants displayed increased electron transport and CO_2 fixation rates in fluctuating light, compared to WT siblings, and accumulated about 15% more dry weight than the wild type when plants were grown under field conditions (Kromdijk et al. 2016).

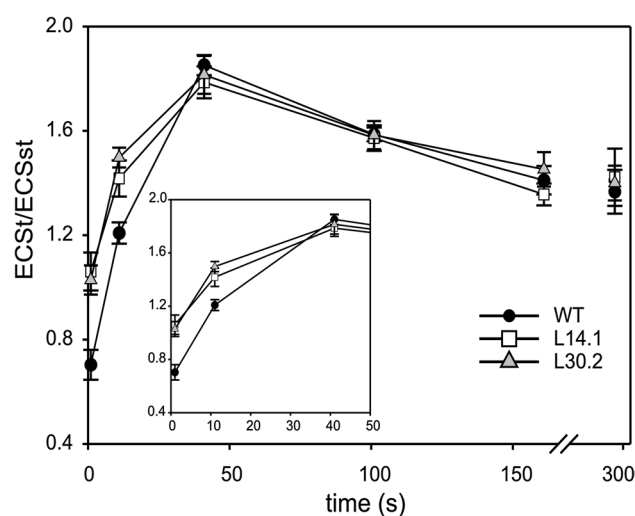


Fig. 6 Enhancement of proton motive force due to Flv proteins in dark-adapted tobacco leaves. Time course of PMF increase estimated on WT (black circles) and Flv-expressing lines L14.1 (white squares) and L30.2 (gray triangles) by measuring the total electrochromic shift (ECS_t) normalized to ΔA_{525} induced by a single-turnover flash on dark-adapted leaves (ECS_{st}). Means \pm SE, $n=10$. The inset shows initial values in an expanded time-frame

Pseudocyclic electron flow to oxygen, mediated by Flv proteins, is another strategy to cope with light fluctuations found in cyanobacteria and other phototrophs, but not in angiosperms. This system can alleviate photodamage by transferring reducing equivalents from NADPH to oxygen avoiding over-reduction of the PETC (Allahverdiyeva et al. 2015). We focused on the effect of these flavoproteins on LET, and particularly on PSII protection by NPQ mechanisms, which can be monitored by fluorescence changes in PSII. During photosynthesis induction, prior to the complete activation of the NADPH-consuming Calvin–Benson cycle, the expression of Flv proteins in tobacco chloroplasts provided an additional electron sink that kept the PETC in a more oxidized state (Fig. 2). This led to an enhancement of electron transfer efficiency (estimated by the Φ_{PSII} parameter), as well as a faster generation of proton motive force across the thylakoid membrane (Figs. 2, 5, 6). As a result, energy-dependent NPQ processes were activated sooner, preventing over-reduction of the PETC and maintaining higher photochemical performance (Fig. 3). Moreover, the inhibition of PGR5-dependent CET by antimycin A caused an acute drop in photosynthetic parameters related to PSII efficiency (Φ_{PSII} and qL ; Fig. 4 and Supplementary Fig. S2) in WT plants, with this decline being partially protected in Flv-expressing lines. Kanazawa et al. (2017) have reported that photodamage in *Arabidopsis pgr5* mutant is caused by loss of PMF rather than CEF inhibition per se, underscoring the importance of the overall regulatory system induced by ΔpH . Interestingly, NPQ-related parameters which directly

depend on PMF (NPQ, Φ_{NPQ} , and Φ_{NO}) were only marginally affected in the transgenic plants, suggesting that Flv activity could partially compensate for the lack of CET mediated by PGR5 (Fig. 4 c–e and Supplementary Fig. S2 c–e).

Dark–light responses similar to those reported here for Φ_{PSII} and NPQ were observed in Arabidopsis plants expressing FlvA–FlvB, the orthologues of Flv1 and Flv3 present in *P. patens* (Yamamoto et al. 2016). The time-frames analyzed in tobacco (5–40 s, 5-s intervals; Figs. 2, 3) were shorter than those used for Arabidopsis (0–300 s, 20-s intervals; Yamamoto et al. 2016), allowing for a detailed description of the early responses of WT and Flv-expressing plants to the dark–light transition. Components of NPQ could be dissected into various constituents, reflecting different dissipative mechanisms. A fast increase in light-induced NPQ (Φ_{NPQ}) was observed in Flv-expressing lines, with a concomitant reduction of basal dissipative pathways represented by Φ_{NO} (Fig. 3). The up-regulation of Φ_{NPQ} was further studied by relaxation analysis, which showed that Flv proteins boosted the ΔpH -dependent NPQ dissipative pathways, as reflected by the differential enhancement of Φ_{qE} values in the transgenic lines (Fig. 5). In agreement with those observations, Flv-expressing plants displayed consistently higher PMF values than WT siblings (Fig. 6) at short illumination times, indicating that build-up of the proton gradient across the thylakoid membrane was faster in these lines. In Arabidopsis, no significant differences in PMF (represented by the $\text{ECS}_v/\text{ECS}_{st}$ ratio) were observed, but determinations were carried out 2–3 min after the dark–light transition (Yamamoto et al. 2016). Analysis of the time course of $\text{ECS}_v/\text{ECS}_{st}$ increase in tobacco shows that by that time the steady-state condition was already reached, with similar PMF values for WT and transgenic leaves (Fig. 6).

Observations reported in this article, and those of Yamamoto et al. (2016), indicate that the expression of Flv proteins did not affect photosynthetic parameters under steady-state conditions, acting instead as an additional electron sink for light excess dissipation at the beginning of illumination, and probably under stressful conditions that cause a reduction of the activity of the Calvin–Benson pathway. Our data suggest that the expression of Flv proteins in chloroplasts not only provides an electron sink for excess energy, but also promotes the overall regulatory system of photosynthesis by triggering lumen acidification.

Yamamoto et al. (2016) have proposed that the expression of the Flv system in angiosperms could be advantageous to the plant under fluctuating illumination. This effect might improve growth and yield in the field, where changing environmental conditions are the rule. Experiments are currently underway to test this hypothesis by growing WT and transgenic tobacco plants under unfavorable illumination conditions.

Acknowledgements We thank Álvaro Quijano (Universidad Nacional de Rosario, FCAGr, Argentina) for providing the MultispeQ-Beta device. This work was supported by Grants PICT 2014-2496 and PICT 2015-3828 from the National Agency for the Promotion of Science and Technology (ANPCyT, Argentina), by PIP 1075 from the National Research Council of Argentina (CONICET), by the Federal Ministry of Education and Research (BMBF, Germany), and by the Project Management Juelich (PTJ, Germany). RG is a Fellow of the Bunge & Born Foundation. NC and AFL are faculty members of the School of Biochemical and Pharmaceutical Sciences, University of Rosario (Facultad de Ciencias Bioquímicas y Farmacéuticas, Universidad Nacional de Rosario, Argentina) and staff members of the National Research Council (CONICET, Argentina).

Funding The funding were provided by National Agency for the Promotion of Science and Technology (PICT 2014-2496 and PICT 2015-3828), National Research Council of Argentina (PIP 1075), Federal Ministry of Education and Research and Bundesministerium für Bildung und Forschung.

References

- Ahn TK, Avenson TJ, Peers G, Li Z, Dall'Osto L, Bassi R, Niyogi KK, Fleming GR (2009) Investigating energy partitioning during photosynthesis using an expanded quantum yield convention. *Chem Phys* 357:151–158
- Allahverdiyeva Y, Isojärvi J, Zhang P, Aro EM (2015) Cyanobacterial oxygenic photosynthesis is protected by flavodiiron proteins. *Life* 5:716–743
- Asada K (1999) The water–water cycle in chloroplasts: scavenging of active oxygens and dissipation of excess photons. *Annu Rev Plant Biol* 50:601–639
- Baker NR (2008) Chlorophyll fluorescence: a probe of photosynthesis in vivo. *Annu Rev Plant Biol* 59:89–113
- Duffy CD, Ruban AV (2015) Dissipative pathways in the photosystem-II antenna in plants. *J Photochem Photobiol B* 152:215–226
- Ermakova M, Battchikova N, Allahverdiyeva Y, Aro EM (2013) Novel heterocyst-specific flavodiiron proteins in *Anabaena* sp. *PCC 7120*. *FEBS Lett* 587:82–87
- Gallois P, Marinho P (1995) Leaf disk transformation using *Agrobacterium tumefaciens*-expression of heterologous genes in tobacco. In: Jones H (ed) *Methods in molecular biology. Plant gene transfer and expression protocols*, vol 49. Humana Press Inc, Totowa, NJ, pp 39–48
- Gerotto C, Alboresi A, Meneghesso A, Jokel M, Suorsa M, Aro EM, Morosinotto T (2016) Flavodiiron proteins act as safety valve for electrons in *Physcomitrella patens*. *Proc Natl Acad Sci USA* 113:12322–12327
- Giró M, Ceccoli RD, Poli HO, Carrillo N, Lodeyro AF (2011) An in vivo system involving co-expression of cyanobacterial flavodoxin and ferredoxin–NADP⁺ reductase confers increased tolerance to oxidative stress in plants. *FEBS Open Biol* 1:7–13
- Hagemann M, Fernie A, Espie G, Kern R, Eisenhut M, Reumann S, Bauwe H, Weber A (2013) Evolution of the biochemistry of the photorespiratory C2 cycle. *Plant Biol* 15:639–647
- Hope AB, Valente P, Matthews DB (1994) Effects of pH on the kinetics of redox reactions in and around the cytochrome b_f complex in an isolated system. *Photosynth Res* 42:111–120
- Ilík P, Pavlovič A, Kouřil R, Alboresi A, Morosinotto T, Allahverdiyeva Y, Aro EM, Yamamoto H, Shikanai T (2017) Alternative electron transport mediated by flavodiiron proteins is operational in organisms from cyanobacteria up to gymnosperms. *New Phytol* 214:967–972

- Jagannathan B, Shen G, Golbeck JH (2012) The evolution of Type I reaction centers: the response to oxygenic photosynthesis. In: Burnap RL, Vermaas WFJ (eds) Functional genomics and evolution of photosynthetic systems. Springer, pp 285–316
- Jarvis P, Chen L-J, Li H-M, Peto CA, Fankhauser C, Chory J (1998) An Arabidopsis mutant defective in the plastid general protein import apparatus. *Science* 282:100–103
- Joët T, Cournac L, Horvath EM, Medgyesy P, Peltier G (2001) Increased sensitivity of photosynthesis to antimycin A induced by inactivation of the chloroplast *ndhB* gene. Evidence for a participation of the NADH-dehydrogenase complex to cyclic electron flow around photosystem I. *Plant Physiol* 125:1919–1929
- Kanazawa A, Ostendorf E, Kohzuma K, Hoh D, Strand D, Sato-Cruz M, Savage L, Cruz J, Fisher N, Froehlich J, Kramer D (2017) Chloroplast ATP synthase modulation of the thylakoid proton motive force: implications for Photosystem I and Photosystem II photoprotection. *Front Plant Sci*. doi:10.3389/fpls.2017.00719
- Kramer DM, Evans JR (2011) The importance of energy balance in improving photosynthetic productivity. *Plant Physiol* 155:70–78
- Kramer DM, Johnson G, Kiirats O, Edwards GE (2004) New fluorescence parameters for the determination of Q A redox state and excitation energy fluxes. *Photosynth Res* 79:209–218
- Kromdijk J, Głowacka K, Leonelli L, Gabilly ST, Iwai M, Niyogi KK, Long SP (2016) Improving photosynthesis and crop productivity by accelerating recovery from photoprotection. *Science* 354:857–861
- Kuhlgert S, Austic G, Zegarac R, Osei-Bonsu I, Hoh D, Chilvers MI, Roth MG, Bi K, TerAvest D, Weebadde P (2016) MultispeQ Beta: a tool for large-scale plant phenotyping connected to the open PhotosynQ network. *Royal Soc Open Sci* 3:160592
- Külheim C, Ågren J, Jansson S (2002) Rapid regulation of light harvesting and plant fitness in the field. *Science* 297:91–93
- Müller P, Li X-P, Niyogi KK (2001) Non-photochemical quenching. A response to excess light energy. *Plant Physiol* 125:1558–1566
- Nishio JN, Whitmarsh J (1993) Dissipation of the proton electrochemical potential in intact chloroplasts (II. The pH gradient monitored by cytochrome *f* reduction kinetics). *Plant Physiol* 101:89–96
- Pierella Karlusich JJ, Lodeyro AF, Carrillo N (2014) The long goodbye: the rise and fall of flavodoxin during plant evolution. *J Exp Bot* 65:5161–5178
- Schmittgen T, Livak K (2008) Analyzing real-time PCR data by the comparative CT method. *Nat Protoc* 3:1101–1108
- Shimakawa G, Ishizaki K, Tsukamoto S, Tanaka M, Sejima T, Miyake C (2017) The liverwort, *Marchantia*, drives alternative electron flow using a flavodiiron protein to protect PSI. *Plant Physiol* 173:1636–1647
- Shirao M, Kuroki S, Kaneko K, Kinjo Y, Tsuyama M, Förster B, Takahashi S, Badger MR (2013) Gymnosperms have increased capacity for electron leakage to oxygen (Mehler and PTOX reactions) in photosynthesis compared with angiosperms. *Plant Cell Physiol* 54:1152–1163
- Sugimoto K, Okegawa Y, Tohri A, Long TA, Covert SF, Hisabori T, Shikanai T (2013) A single amino acid alteration in PGR5 confers resistance to antimycin A in cyclic electron transport around PSI. *Plant Cell Physiol* 54:1525–1534
- Takahashi S, Badger MR (2011) Photoprotection in plants: a new light on photosystem II damage. *Trends Plant Sci* 16:53–60
- Vicente JB, Gomes CM, Wasserfallen A, Teixeira M (2002) Module fusion in an A-type flavoprotein from the cyanobacterium *Synechocystis* condenses a multiple-component pathway in a single polypeptide chain. *Biochem Biophys Res Comm* 294:82–87
- Vicente JB, Justino MC, Gonçalves VL, Saraiva LM, Teixeira M (2008) Biochemical, spectroscopic, and thermodynamic properties of flavodiiron proteins. *Methods Enzymol* 437:21–45
- Yamamoto H, Takahashi S, Badger MR, Shikanai T (2016) Artificial remodelling of alternative electron flow by flavodiiron proteins in Arabidopsis. *Nat Plants*. doi:10.1038/nplants.2016.12
- Yamori W, Shikanai T (2016) Physiological functions of cyclic electron transport around photosystem I in sustaining photosynthesis and plant growth. *Ann Rev Plant Biol* 67:81–106
- Zhu XG, Ort DR, Whitmarsh J, Long SP (2004) The slow reversibility of photosystem II thermal energy dissipation on transfer from high to low light may cause large losses in carbon gain by crop canopies: a theoretical analysis. *J Exp Bot* 55:1167–1175